Benchmarking the codes VORPAL, OSIRIS, and QuickPIC with Laser Wakefield Acceleration Simulations

K. Paul*, C. Huang†, D. L. Bruhwiler*, W. B. Mori†, F. S. Tsung†,
E. Cormier-Michel**, C. G. R. Geddes**, B. Cowan*, J. R. Cary*,
E. Esarey**, R. A. Fonseca‡, S. F. Martins‡ and L. O. Silva‡

*Tech-X Corporation, Boulder, CO, USA
†University of California at Los Angeles, Los Angeles, CA, USA
**Lawrence Berkeley National Laboratory, Berkeley, CA, USA
‡GoLP/Instituto de Plasmas e Fusão Nuclear, Instituto Superior Técnico, Lisboa, Portugal

Abstract. Three-dimensional laser wakefield acceleration (LWFA) simulations have recently been performed to benchmark the commonly used particle-in-cell (PIC) codes VORPAL, OSIRIS, and QuickPIC. The simulations were run in parallel on over 100 processors, using parameters relevant to LWFA with ultra-short Ti-Sapphire laser pulses propagating in hydrogen gas. Both first-order and second-order particle shapes were employed. We present the results of this benchmarking exercise, and show that accelerating gradients from full PIC agree for all values of a_0 and that full and reduced PIC agree well for values of a_0 approaching 4.

Keywords: laser-plasma accelerators, simulation, benchmarking
PACS: 01.30.Cc, 02.70.Bf, 52.38.Kd, 52.65.Rr

INTRODUCTION

VORPAL [1], OSIRIS [2], and QuickPIC [3] are well-established particle-in-cells code used for simulating a variety of laser-plasma problems [4, 5, 6, 7, 8, 9, 10]. OSIRIS and VORPAL are fully-explicit particle-in-cell (PIC) codes developed by groups at UCLA/IST/USC and Tech-X Corporation, respectively. QuickPIC is a quasi-static particle-in-cell code developed by UCLA/U. of Maryland/IST/USC. While these three codes have been widely used throughout the plasma physics community, they have not been benchmarked against each other in detail until now.

An early attempt at benchmarking OSIRIS and VORPAL was done at the 2004 Advanced Accelerator Concepts Workshop [11]. This benchmarking effort conducted 2D laser wakefield acceleration simulations with both OSIRIS and VORPAL. The results showed significant differences that were attributed to differing laser pulse profiles, differing pulse launch methods, varying plasma parameters, boundary conditions, and particle loading methods. The conclusion of this brief study was that a more detailed benchmarking effort should be done, addressing all of these differences with an eye to the details.

This article presents the efforts made by UCLA, IST, Tech-X Corporation, and LBNL to address the significant differences found in the previous benchmarking effort, extending the comparison to include QuickPIC and with full 3D simulations. In the following sections, we compare the three codes in a common laser wakefield acceleration (LWFA)

CP1086, *Advanced Accelerator Concepts: 13th Workshop,* edited by C. B. Schroeder, W. Leemans, and E. Esarey

TABLE 1. Laser and plasma parameters used in the laser wakefield acceleration benchmarking simulations.

Normalized Vector Potential of Laser (a_0)	Laser Wavelength (λ_0)	Laser Pulse Length (Δt_0)	Laser Pulse Width (W_0)	Plasma Density (n_0)
0.5, 1.0, 2.0, 4.0	0.8 μm	15 fs	8.2 μm	1.38×10^{19} cm^{-3}

TABLE 2. Grid and simulations parameters used by the explicit PIC codes, VORPAL and OSIRIS, in the laser wakefield acceleration benchmarking simulations.

Transverse Box Size (Square)	Longitudinal Box Size	Grid Size in Cells (Cubed)	Transverse Cell Size (Square)	Longitudinal Cell Size	Time Step Size	Number of Time Steps
81.52 μm	20.5 μm	512^3	0.16 μm	0.04 μm	0.1 fs	1600

scenario. The next section describes the benchmarking parameters in a case relevant to LWFA with Ti-Sapphire lasers propagating in hydrogen gas. The following section details comparisons of the laser and wake fields in the plasma, showing very good agreement between the three codes.

BENCHMARKING PARAMETERS

Table 1 shows the laser and plasma parameters used in the benchmarking simulations. Four different laser strengths are considered, $a_0 = 0.5, 1.0, 2.0, 4.0$, scanning over the range from weakly to moderately non-linear dynamics. Planned experiments at LBNL will operate well within this range of laser intensities. The longitudinal and transverse profile of the laser is the same as given in [7], which uses a polynomial longitudinal profile that smoothly goes to zero in a finite distance.

Table 2 shows the grid and simulation parameters used by the explicit PIC codes, VORPAL and OSIRIS. QuickPIC uses the same transverse cell size and transverse box size, but the longitudinal cell size is increased to $1.07\frac{\lambda_0}{2\pi}$, satisfying the $\frac{2\pi dz}{\lambda_0} > 1$ condition for stability. There are only two time steps in the QuickPIC simulation, each with a length of 80 fs.

The laser pulse starts in vacuum, adjacent and about to enter a plasma region with no density ramp. The laser pulse is allowed to travel for 160 fs into the plasma, or slightly less than 50 μm. This gives the laser pulse time to propagate a few plasma wavelengths, far enough into the plasma for the wake to fully form behind the pulse.

All three codes use a moving window approach, where the simulation box moves at the speed of light. However, since the speed of the pulse is slightly less than light speed, the laser pulse will drift back very slightly in the window after the 160 fs duration of the simulation. Both QuickPIC and OSIRIS initialize the pulse near the edge of the simulation domain, the edge toward which the pulse is propagating, and the moving window starts with the first time step of the simulation. VORPAL, however, launches its pulse from a surface using time-dependent boundary conditions with the moving

window turned off. When the VORPAL laser pulse reaches the far edge of the domain, the moving window turns on. Once the moving window engages—in all three codes—plasma begins sweeping into the domain. In QuickPIC, the plasma sweeps by the laser under the quasi-static approximation.

First-order particle shapes (*i.e.*, linear field interpolation and current deposition) were used for simulations with $a_0 = 0.5, 1, 2, 4$ in the explicit PIC codes. QuickPIC deposits the current and charge, and hence its particle shapes are one order higher than those in the local charge conserving schemes used in VORPAL and OSIRISÀ 4-pass 1–2–1 digital filter, with 1 pass of compensation, was used to smooth all of the current components along the longitudinal direction. Additionally, second-order particles shapes were used for $a_0 = 1, 2, 4$ in the explicit PIC codes. No smoothing was done with the second-order particle shapes. All of these simulation used 8 particles per cell.

No attempt was made to exactly match the phase of the laser pulse in the explicit PIC codes. Since the wake is formed from the ponderomotive force, it is reasonable to assume that the phase of the laser pulse will have little effect on the shape of the wake behind the pulse. This fact—as well as the fundamental differences between the three codes in launching the laser pulse and setting up the simulation domain and grid—makes precise positioning of the laser pulse in the simulation domain at the end of the simulation difficult. Hence, we assume that there is an unknown longitudinal offset between the data produced by the three codes, which we correct for in the resulting comparison plots.

RESULTS

To compare the codes, we look at the electric fields in the direction of the laser pulse polarization and in the direction of the pulse propagation, which is a part of the wake produced by the laser pulse. These components we refer to as the *laser field* and the *wake field*, respectively. We then directly compare 1D line-outs of the fields down the center of the simulation along the axis of propagation of the laser pulse. To determine the unknown longitudinal offset, we aligned the profiles of the wake fields behind the laser pulse in the lowest a_0 simulation, where we expect all three codes to agree very well. This determines the longitudinal offset, which we apply to all of the rest of the data in all of the simulations, $a_0 = 0.5, 1, 2, 4$.

The explicit PIC codes interpolate fields directly from the Yee mesh when computing the particle push. This is always done in OSIRIS. VORPAL normally interpolates the nodal fields for the particle push, but VORPAL is capable of interpolating directly from the Yee mesh, which is the option used in this exercise. Thus, the fields compared from the full PIC cases are the fields from the Yee mesh, which are the same fields used to compute the particle kinetics. QuickPIC is a spectral code so all fields are defined at the nodes.

Figure 1 shows the 1D line-outs of the laser field and wake field for the $a_0 = 2, 4$ cases after 1600 times steps (160 fs) from the moment the laser pulse strikes the edge of the plasma. These results are with first-order particle shapes. The laser pulse plots are only shown for the explicit PIC codes, OSIRIS and VORPAL. The slight differences for QuickPIC at $a_0 = 2$ are believed to be the effects of boundary conditions with the

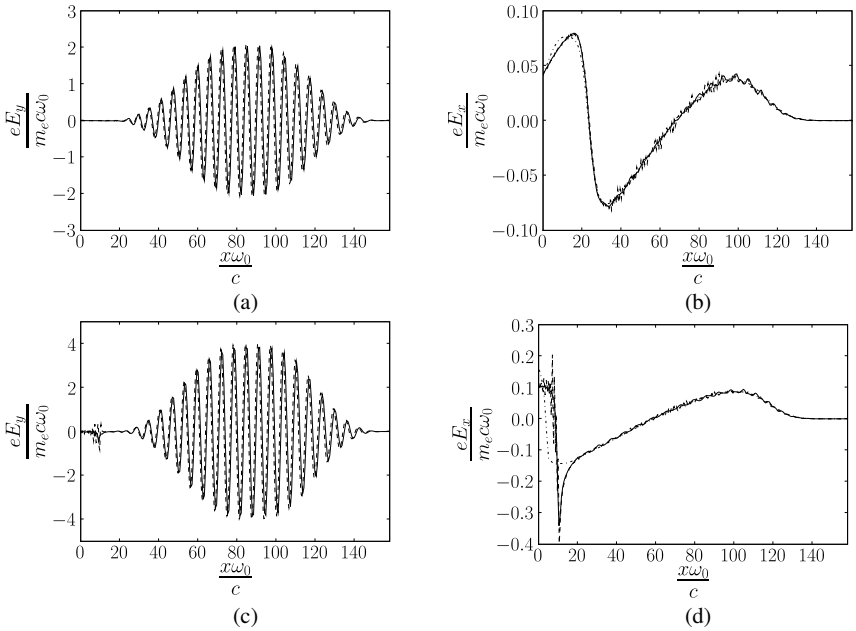

FIGURE 1. The electric field in the direction of laser polarization (left plots) and in the direction of laser propagation, or wake field, (right plots) with first-order particle shapes. Figures (a) and (b) are for $a_0 = 2$, and figures (c) and (d) are for $a_0 = 4$. OSIRIS data is shown with the solid lines. VORPAL data is shown with the dashed lines. QuickPIC data (shown only on the right) is shown with dash-dot lines. While not shown, there is excellent agreement for the $a_0 = 0.5$ and $a_0 = 1$ cases.

solver, and the differences at $a_0 = 4$ are believed to be due to particle trapping. Note that if a trailing particle beam is loaded into the wake that it would normally be added at locations in the wake where the agreement between the full PIC and quasi-static PIC is still excellent even for this value of a_0 . Up to a small phase difference in the laser pulse, the explicit PIC codes agree very well for all values of a_0. While not shown, all three codes agree excellently for $a_0 = 0.5, 1$. Two-dimensional contour plots of the wake fields are shown for $a_0 = 4$ in Figure 3.

For the second-order particle shapes—which have been shown to reduce certain kinetic errors [12]—the $a_0 = 1, 2, 4$ cases were performed with VORPAL and OSIRIS. Figure 2 shows the laser and wake fields for runs with second-order particle shapes for $a_0 = 2, 4$. The laser phase difference seen between the two codes is larger, closer to π, but the agreement in the wake fields is still very good. One can see a slight difference in the location of the wake for $a_0 = 4$, but agreement is excellent for lower values of a_0. Figure 4 shows the 2D contour plots of the wake fields for $a_0 = 4$.

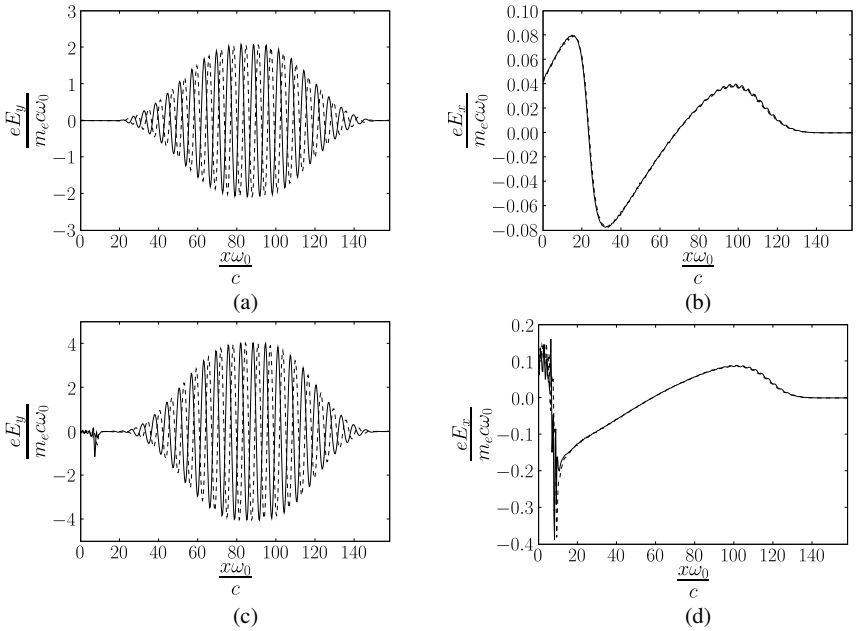

FIGURE 2. The electric field in the direction of laser polarization (left plots) and in the direction of laser propagation, or wake field, (right plots) with second-order particle shapes. Figures (a) and (b) are for $a_0 = 2$, and figures (c) and (d) are for $a_0 = 4$. OSIRIS data is shown with the solid lines. VORPAL data is shown with the dashed lines. While not shown, agreement is excellent for $a_0 = 1$, as well.

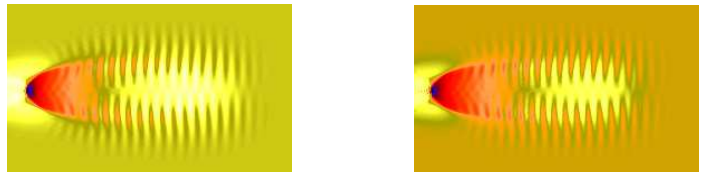

FIGURE 3. Contour plots of the wake fields produced by OSIRIS (a) and VORPAL (b) for $a_0 = 4$ with first-order particle shapes (*i.e.*, first-order field interpolation and first-order current deposition).

CONCLUSIONS

The exercise performed in this paper compares the laser and wake fields produced by a short pulses propagating a small distance into the plasma. We find that the fields generated by all three codes agree very well for these simple LWFA simulations. For low values of a_0 (*i.e.*, $a_0 < 2$), the quasi-static code QuickPIC shows excellent agreement with the explicit PIC codes, VORPAL and OSIRIS. For larger values of a_0, effects from boundary conditions and the onset of particle trapping lead to differences between QuickPIC and the explicit PIC codes. However, for all values of a_0 simulated, the

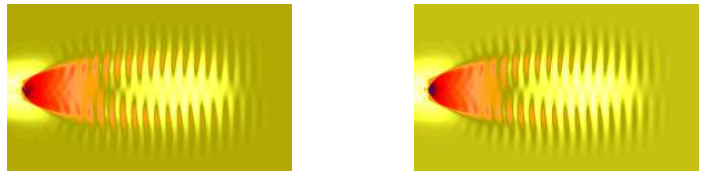

(a) (b)

FIGURE 4. Contour plots of the wake fields produced by OSIRIS (a) and VORPAL (b) for $a_0 = 4$ with second-order particle shapes (*i.e.*, second-order field interpolation and second-order current deposition).

explicit PIC codes agree very well with each other.

This marks the successful conclusion of the first benchmarking effort with the three codes, VORPAL, OSIRIS, and QuickPIC. A more thorough comparison of the codes might include comparisons of the dispersion relation and pulse evolution for long propagation distances, particle trapping, and other kinetic phenomena. Such comparisons will assuredly take place in future benchmarking efforts.

ACKNOWLEDGMENTS

This research used resources of the National Energy Research Scientific Computing Center, and is supported by the U.S. Department of Energy, under the Office of Science contracts #DE-FC02-07ER41499 and #DE-AC02-05CH11231, and under the contracts #DE-FG03-92ER40727, #DE-FG52-06NA26195, #DE-FC02-07ER41500, and #DE-FG02-03ER54721, the National Science Foundation contract #NSF-Phy-0321345, and by Tech-X Corporation.

Thanks, also, to the rest of the VORPAL development team, including T. Austin, G. I. Bell, R. S. Busby, J. Carlsson, D. A. Dimitrov, A. Hakim, J. Loverich, P. Messmer, P. J. Mullowney, C. Nieter, S. W. Sides, N. D. Sizemore, D. N. Smithe, P. H. Stoltz, S. A. Veitzer, D. J. Wade-Stein, G. R. Werner, M. Wrobel, N. Xiang, and W. Ye.

REFERENCES

1. C. Nieter, and J. R. Cary, *J. Comp. Phys.* **196**, 448–472 (2004).
2. R. A. Hemker, et al., *Lecture Notes in Computational Science* **2331**, 342–351 (2002).
3. C. K. Huang, et al., *J. Comp. Phys.* **217**, 658–679 (2006).
4. C. G. R. Geddes, et al., *Nature* **431**, 538–541 (2004).
5. C. G. R. Geddes, et al., *PRL* **100**, 215004 (2008).
6. S. P. D. Mangles, et al., *Nature* **431**, 535 (2004).
7. F. S. Tsung, et al., *Physics of Plasmas* **13**, 056708 (2006).
8. C. G. R. Geddes, et al., *J. Physics: Conf. Series* **125**, 12002/1–11 (2008).
9. J. M. Vieira, et al., *IEEE Transactions on Plasma Science* **36**, 1722–1727 (2008).
10. I. Blumenfeld, et al., *Nature* **445**, 741–744 (2007).
11. J. R. Cary, and C. L. Bohn, "Computational Accelerator Physics Working Group Summary," in *Proceedings for the Eleventh Advanced Accelerator Physics Workshop*, edited by V. Yamimenko, American Institute of Physics, 2004.
12. E. Michel, et al., *Phys. Rev. E* **78**, 016404 (2008).